

See discussions, stats, and author profiles for this publication at: <https://www.researchgate.net/publication/258521821>

# Bimolecular Auger Recombination of Electron–Hole Pairs in Two-Dimensional CdSe and CdSe/CdZnS Core/Shell Nanoplatelets

ARTICLE in JOURNAL OF PHYSICAL CHEMISTRY LETTERS · OCTOBER 2013

Impact Factor: 7.46 · DOI: 10.1021/jz401970p

CITATIONS

27

READS

55

8 AUTHORS, INCLUDING:



**Mickael D Tessier**

Ghent University

14 PUBLICATIONS 343 CITATIONS

SEE PROFILE



**F.C. Grozema**

Delft University of Technology

129 PUBLICATIONS 3,721 CITATIONS

SEE PROFILE



**Juleon M Schins**

Delft University of Technology

79 PUBLICATIONS 2,558 CITATIONS

SEE PROFILE



**Laurens D A Siebbeles**

Delft University of Technology

249 PUBLICATIONS 7,267 CITATIONS

SEE PROFILE

# Bimolecular Auger Recombination of Electron–Hole Pairs in Two-Dimensional CdSe and CdSe/CdZnS Core/Shell Nanoplatelets

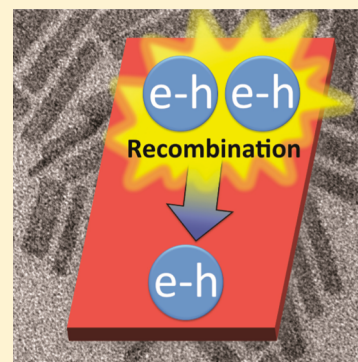
Lucas T. Kunneman,<sup>†</sup> Mickael D. Tessier,<sup>‡</sup> Hadrien Heuclin,<sup>‡</sup> Benoit Dubertret,<sup>‡</sup> Yaroslav V. Aulin,<sup>†</sup> Ferdinand C. Grozema,<sup>†</sup> Juleon M. Schins,<sup>\*,†</sup> and Laurens D. A. Siebbeles<sup>\*,†</sup>

<sup>†</sup> Optoelectronic Materials Section, Department of Chemical Engineering, Delft University of Technology, Julianalaan 136, 2628 BL Delft, The Netherlands

<sup>‡</sup> Laboratoire de Physique et d'Etude des Matériaux, CNRS, Université Pierre et Marie Curie, ESPCI, 10 rue Vauquelin, 75005 Paris, France

## S Supporting Information

**ABSTRACT:** We have determined the Auger recombination kinetics of electrons and holes in colloidal CdSe-only and CdSe/CdS/ZnS core/shell nanoplatelets by time-resolved photoluminescence measurements. Excitation densities as high as an average of 18 electron–hole pairs per nanoplatelet were reached. Auger recombination can be described by second-order kinetics. From this we infer that the majority of electrons and holes are bound in the form of neutral excitons, while the fraction of free charges is much smaller. The biexciton Auger recombination rate in nanoplatelets is more than 1 order of magnitude smaller than for quantum dots and nanorods of equal volume. The latter is of advantage for application in lasers, light-emitting diodes, and photovoltaics.



**SECTION:** Physical Processes in Nanomaterials and Nanostructures

Colloidal semiconductor nanocrystals have fascinating optical and electronic properties that are distinct from bulk materials.<sup>1,2</sup> The possibility to tune the optoelectronic properties by adjustment of nanocrystal composition, size, or shape offers tremendous prospects for application in, e.g., transistors, light-emitting diodes, photovoltaic devices, lasers, solar fuel production, and biolabeling.<sup>1,3,4</sup> Spherical quantum dots and one-dimensional nanorods have been the subject of intense research during the past decade.<sup>1,2,5,6</sup> In the past few years, the synthesis of flat colloidal two-dimensional metal-chalcogenide nanoplatelets with a thickness of only a few atomic layers has been developed.<sup>7</sup> The small thickness of such two-dimensional semiconductor materials gives rise to effects of quantum confinement on the properties of electronic excited states (excitons) and excess charge carriers.<sup>7,8</sup> Indeed, the optical absorption bands and fluorescence spectrum of nanoplatelets exhibit a pronounced blue-shift as nanoplatelet thickness is reduced.<sup>9–12</sup> The thickness can be controlled with atomic precision, as has been confirmed by the observation that the photoluminescence characteristics of an ensemble of CdSe nanoplatelets coincides with that of a single nanoplatelet.<sup>13</sup> Compared to strongly quantum-confined spherical CdSe and CdTe quantum dots,<sup>14</sup> the platelets exhibit much narrower absorption and photoluminescence peaks, smaller Stokes shift, higher radiative rate (more than an order of magnitude higher) and high photoluminescence quantum yield (close to 50%).<sup>9,10,12,13</sup> The kinetics of cooling of multiple hot

electron–hole pairs in CdSe nanoplatelets was found to be similar to that for bulk material and unlike that for charges in quantum dots or nanorods.<sup>11</sup> The recent studies mentioned above demonstrate that the optoelectronic properties of two-dimensional CdSe nanoplatelets are very distinct from zero-dimensional quantum dots and one-dimensional nanorods.

To date, it has not been established to which extent electrons and holes in colloidal CdSe nanoplatelets exist as Coulombically bound pairs in the form of excitons, rather than free charges that move independently. The character of electron–hole pairs determines the recombination kinetics of multiple electron–hole pairs. We studied the character of electrons and holes by monitoring their recombination kinetics. Insight into the mechanism of recombination is important, since recombination causes unwanted carrier loss in light-emitting diodes at high current,<sup>15</sup> in quantum dot solar cells exploiting carrier multiplication,<sup>16</sup> and in nanocrystal lasers.<sup>17</sup>

Multiple electron–hole pairs can decay via an Auger process in which an electron and hole recombine and transfer their energy by re-exciting a third particle, either an electron or a hole.<sup>18</sup> In the case that electrons and holes act as uncorrelated particles, Auger recombination follows cubic (third-order) kinetics. This occurs in two situations: first in bulk semi-

**Received:** September 13, 2013

**Accepted:** October 9, 2013

**Published:** October 9, 2013

conductors with small exciton binding energy, such that free charges form the majority of the photoexcited species; second, in nanocrystals in the strong confinement regime, when the average mutual distance between an electron and a hole is comparable to the nanocrystal size. On the other hand, second-order kinetics occurs when two conditions are satisfied: excitons are the majority photoexcited species, and the Bohr radius is much smaller than the nanocrystal size. Indeed, in small spherical CdSe quantum dots Auger recombination follows cubic kinetics, while bimolecular recombination occurs in longer CdSe nanorods.<sup>19</sup> Such a transition is expected when the length of a nanorod exceeds the exciton Bohr radius, which is 5.4 nm in bulk CdSe. The question remains to which extent electron–hole pairs in colloidal CdSe nanoplatelets have the character of excitons rather than free charges.

We studied decay kinetics of multiple electron–hole pairs in CdSe nanoplatelets by time-resolved photoluminescence spectroscopy, with excitation densities as high as 18 electron–hole pairs on average per nanoplatelet. The results indicate that excitons are the majority photoexcited species, decaying via second order Auger recombination. Similar studies have also been conducted with transient absorption (TA) spectroscopy. Whereas in TA experiments the bleach signal saturates for high excitation densities, such a saturation does not occur in photoluminescence.

Besides CdSe-only nanoplatelets, we also studied CdSe/CdS/ZnS core/shell/shell heteronanoplatelets, which are analogous to those in ref 20. Passivation with a shell enhances the fluorescence quantum yield and photostability and reduces blinking.<sup>21</sup> Extension of the electron wave function into the shell can suppress Auger recombination and exciton formation. We found that Auger recombination can be described by second-order kinetics that is similar for the CdSe-only and the heteronanoplatelets. This implies that electron–hole pairs predominantly exist in the form of excitons and that the fraction of free charge carriers is much smaller. We found that Auger recombination of biexcitons in nanoplatelets is more than an order of magnitude slower than in spherical quantum dots or nanorods with equal volume.

Zinc blende CdSe-only nanoplatelets were synthesized as described by Ithurria et al.<sup>9</sup> The thickness is 1.5 nm, corresponding to 5 monolayers of CdSe, as determined by TEM.<sup>20</sup> The average lateral extensions are 6–7 nm and 30–35 nm. The CdSe/CdS/ZnS core/shell nanoplatelets were synthesized as described by Mahler et al.<sup>20</sup> The thickness of the CdSe core is 1.2 nm, corresponding to 4 monolayers of CdSe. The core was overcoated on each side with three monolayers of CdS and 2.5 monolayers of ZnS, resulting in a total thickness of 4.3 nm. The average lateral extensions are 9–12 nm and 20–24 nm. The nanoplatelets were suspended in hexane and kept airtight in 10 mm × 10 mm cuvettes (QS Hellma, filled under N<sub>2</sub> atmosphere) during all optical measurements. The optical density of the samples at 400 nm was 0.23 for CdSe-only and 0.10 for the core/shell nanoplatelets, which is sufficiently low such that the excitation density is nearly homogeneous and reabsorption of photoluminescence does not contribute significantly to the signals.

Figure 1 shows the absorption and photoluminescence emission spectra of the nanoplatelets (measured with Elmer Pelkin L900 and PTI Quantamaster). The absorption spectra exhibit distinct narrow peaks, which are typical for atomically flat nanoplatelets.<sup>7,9</sup> The first peak at the lowest energy is due to excitation of an electron from the heavy-hole valence band to

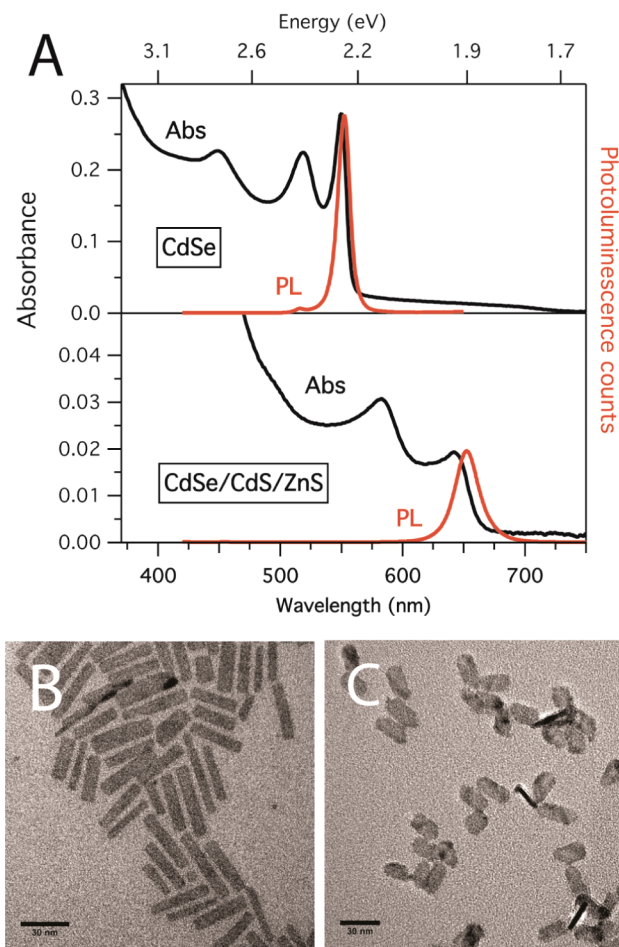


**Figure 1.** (A) Absorption (black) and photoluminescence (red) spectra of CdSe-only (top) and CdSe/CdS/ZnS (bottom) nanoplatelets. The well-resolved absorption peaks and narrow photoluminescence spectra reflect that the nanoplatelets are atomically flat. The path length was 10 mm, and the excitation wavelength for photoluminescence was 400 nm. TEM images of the CdSe-only and CdSe/CdS/ZnS nanoplatelets are shown in B and C, respectively.

the conduction band, followed by the light-hole to conduction band excitation. The third peak in the absorption spectrum of the CdSe-only nanoplatelets is attributed to excitation from the spin–orbit split-off band to the conduction band. The photoluminescence spectra show a small Stokes shift and peak at 553 nm for the CdSe-only nanoplatelets and 653 nm for the core/shell nanoplatelets. The redshift of the absorption and photoluminescence spectra of the core–shell nanoplatelets with respect to the CdSe-only nanoplatelets is attributed to partial delocalization of the electron into the CdS shell.<sup>21</sup>

The decay kinetics of (multiple) electron–hole pairs was monitored by time-resolved photoluminescence measurements, using an ultrafast Ti:sapphire laser (Chameleon Ultra by Coherent Inc.), and a Hamamatsu C5680 streak camera. The laser produces 150 fs pulses at an 80 MHz repetition rate, centered around 800 nm. The nanoplatelets were photoexcited using pump light of 400 nm, which was generated by second harmonic generation. A pulse picker (Angewandte Physik & Elektronik) was used to decrease the pump repetition rate to 4 MHz. The pump beam was focused on the sample with a 50 mm focal length lens. The resulting focus is slightly elliptical, with main axes of 18 and 12  $\mu$ m full width at half-maximum (measured using a Thorlabs beam profiler BC106-VIS). In this

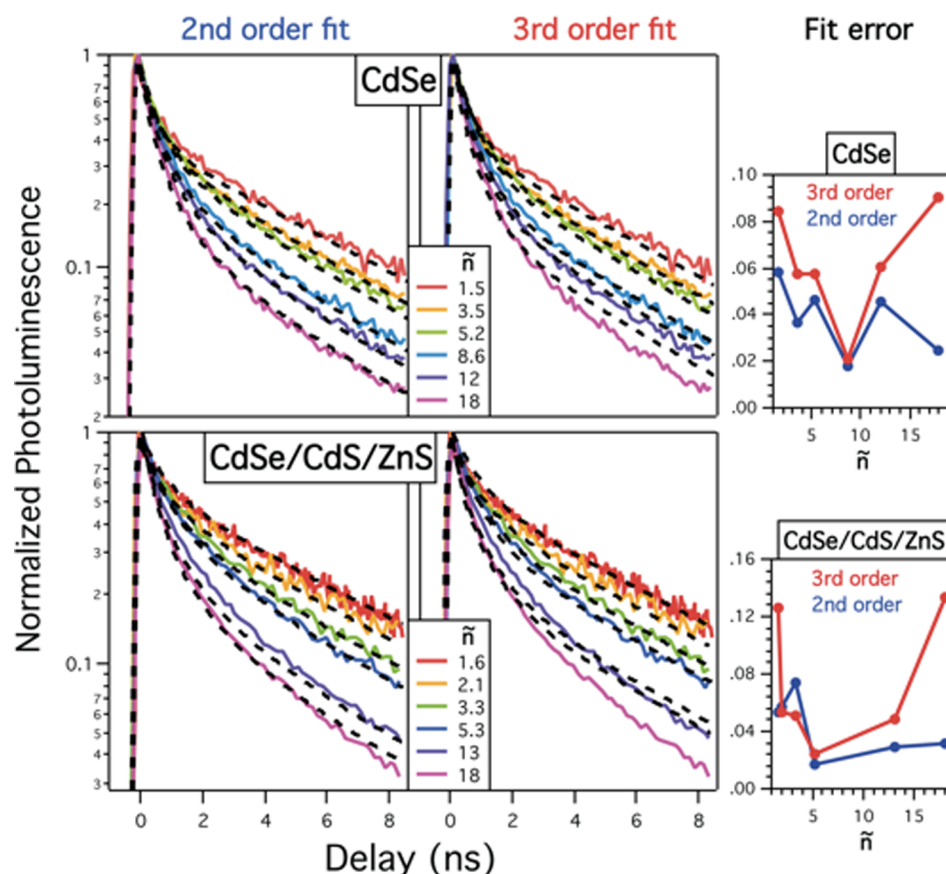


**Figure 2.** Photoluminescence normalized to the maximum in the transient for CdSe-only (top row) and CdSe/CdS/ZnS core/shell nanoplatelets (bottom row). The experimental data are presented identically in the left and middle columns. In the left column, the second-order global fit is shown, whereas the middle column shows the third-order global fit. The rightmost column shows the fit error as a function of average occupation, for both the second and third order fit. Clearly, both samples show a second-order Auger decay typical for electron–hole pairs that are Coulombically bound in the form of excitons.

focus, the maximum pump power of 3 mW corresponds to a peak fluence of  $6.0 \times 10^{14}$  photons/cm<sup>2</sup>/pulse. Photoluminescence of the nanoplatelets was collected at a right angle to the pump-beam propagation by means of a 200 mm focal length lens. The data discussed below were obtained by photoexciting the nanoplatelets with horizontally polarized pump light. The photoluminescence decay kinetics was found to be identical for horizontally and vertically polarized pump light, which implies that rotational diffusion of the nanoplatelets plays no role. The alignment was adjusted such that the measured photoluminescence decay rate is maximum. This ensures that the focus of the pump beam is imaged on the spectrograph. The entrance slit of the spectrograph (Princeton Instruments Acton SP2300) has a width of 100  $\mu$ m. The streak camera was operated in the photon counting and slow sweep mode, which resulted in a rise time of 150 ps. The time-dependent photoluminescence signals shown below are all obtained after (i) spectral integration over the photoluminescence peak, and (ii) subtraction of a baseline measured at times prior to excitation. The baseline is due to dark counts in the streak camera, i.e., a background signal unrelated to the sample. The pump power was varied using a continuously variable neutral density filter.

The pump laser fluence varies over the detection volume. In the theoretical modeling of the data this variation was taken into account, as detailed in the Supporting Information. As only excited nanoplatelets contribute to photoluminescence, an

appropriate measure for the level of nanoplatelet excitation is  $\tilde{n}$ , the average number of electron–hole pairs *per excited nanoplatelet*. Note that a direct result of this definition is that  $\tilde{n} \geq 1$ , i.e., an excited nanoplatelet contains, by definition, at least one electron–hole pair. To obtain  $\tilde{n}$ , a weighted average of the Poisson distribution over the pump beam profile is calculated, as described in the Supporting Information. To study the kinetics of Auger recombination, we varied the pump fluence to obtain an average number of electron–hole pairs per excited nanoplatelet,  $\tilde{n}$ , between 1.5 and 18. The photoluminescence data on both the CdSe-only and the CdSe core/shell-nanoplatelets are shown in Figure 2, in the top and bottom rows, respectively.

The vertical axis shows the normalized photoluminescence, which is directly proportional to the instantaneous number of electron–hole pairs. For the CdSe-only nanoplatelets, the photoluminescence per pump photon does not depend on pump fluence, which suggests that no recombination occurs within the experimental time resolution (150 ps). The photoluminescence transient in the limit of low pump fluence ( $\tilde{n} = 1.5$ ) can be described by the sum of two exponentially decaying functions with a short (470 ps) and a long (6.2 ns) lifetime. This multiexponential decay is known to occur in individual CdSe nanoplatelets at room temperature, and has been attributed to the presence of different emitting states.<sup>13</sup> For increasing pump power the initial decay becomes faster, which we attribute to Auger recombination of electrons and holes.



The photoluminescence transients of the core/shell nanoplatelets are similar to those of the CdSe-only nanoplatelets, except for two differences. The fast component of the biexponential decay in the core/shell nanoplatelets has slightly longer decay time and has smaller relative amplitude. The longer decay time can result from partial charge separation, as the hole is confined to the CdSe core, while the electron may delocalize into the CdS shell.

The time dependence of the normalized photoluminescence in Figure 2 reflects the population decay of electron–hole pairs. To determine whether the decay involves second or third order Auger recombination, we modeled the photoluminescence data by a stochastic cascade model.<sup>22,23</sup> The time-dependent probability  $\rho_n(t)$  that a nanoplatelet contains  $n \geq 1$  electron–hole pairs is obtained from the kinetic equation

$$\frac{d}{dt}\rho_n(t) = -\frac{\rho_n(t)}{\tau_n} + \frac{\rho_{n+1}(t)}{\tau_{n+1}} \quad (1)$$

$$\frac{1}{\tau_n} = nk_{\text{lin}} + k_n^{[m]} \quad (2)$$

$$k_n^{[m]} = \left(\frac{n}{2}\right)^{m-1} (n-1)k_2^{[m]} \quad (3)$$

with  $\tau_n$  the lifetime for decay of a nanoplatelet with  $n$  electron–hole pairs to a state with  $n-1$  pairs,  $k_{\text{lin}}$  the decay rate of a single electron–hole pair, and  $k_n^{[m]}$  the Auger recombination rate of  $n$  electron–hole pairs via a process of order  $m$ . The set of coupled differential equations described by eqs 1–3 was solved analytically, as described in the Supporting Information. The initial population of electron–hole pairs in a nanoplatelet was calculated from a Poisson distribution, taking into account the variation of the pump laser fluence over the volume probed by the photoluminescence measurements. The photoluminescence is proportional to the total number of excitations,  $\sum n\rho_n(t)$ , as detailed in the Supporting Information. As mentioned in the previous section, the biexponential decay of the nanoplatelets is due to the presence of different emitting states. We took the latter into account by including a fraction  $f$  of nanoplatelets with fast linear decay and a fraction  $1-f$  with slow linear decay. The fraction  $f$  was treated as fit parameter. The other fit parameters are the three decay rates  $k_{\text{lin, slow}}$ ,  $k_{\text{lin, fast}}$  and  $k_2^{[m]}$ .

The results of global fits to photoluminescence transients at different pump intensities are shown as dashed curves in Figure 2 for second (left column) and third-order Auger recombination (right column). The rightmost column in Figure 2 shows that for both types of nanoplatelets, the quality of the global fit is highest for second order Auger recombination. The fit error was calculated by summing the square of the residuals. When comparing the fits to the measurements, it is seen that at higher density of electron–hole pairs, the third-order fit does not reproduce the experimental data, in contrast to the second-order fit. The second-order recombination entails that the electron–hole pairs in both CdSe-only and core/shell nanoplatelets predominantly exist as excitons with Bohr radius smaller than the lateral dimensions of a nanoplatelet, while the amount of free charges is relatively small. It is inferred that the exciton binding energy in a two-dimensional nanoplatelet exceeds thermal energy at room temperature. The Auger decay rates of biexcitons are similar for both nanoplatelets:  $k_2^{[2]} = 0.07 \text{ ns}^{-1}$  and  $0.12 \text{ ns}^{-1}$  for CdSe-only and core/shell-nanoplatelets,

respectively. The rate constants can be compared with each other, since the two types of nanoplatelets studied have similar area.

The fitted linear decay constants are  $k_{\text{lin, slow}} = 0.16 \text{ ns}^{-1}$  for CdSe-only and  $k_{\text{lin, slow}} = 0.15 \text{ ns}^{-1}$  for heteronanoplatelets. For CdSe-only nanoplatelets,  $k_{\text{lin, fast}} = 2.1 \text{ ns}^{-1}$ , while for heteronanoplatelets  $k_{\text{lin, fast}} = 1.6 \text{ ns}^{-1}$ . The fit parameter  $f$ , which splits the fast and slow populations is 0.59 for CdSe-only nanoplatelets, and 0.39 for the heteronanoplatelets. The fits were made using a measured absorption cross of  $1.5 \times 10^{-13} \text{ cm}^2$ . The sensitivity of the fit on the cross-section was checked for a range of cross sections:  $6.7 \times 10^{-14} \text{ cm}^2$  to  $2.5 \times 10^{-13} \text{ cm}^2$ . In all cases the second order fit convincingly outperforms the third order fit. It is interesting to note that the fit was optimal at an order of  $m = 1.8$ , slightly below 2.

We have explained the decay kinetics in terms of exciton–exciton recombination because of the quadratic dependence of the photoluminescence signal on exciton multiplicity. If this recombination process had resulted from a classical exciton diffusion process, a product of reaction radius and diffusion constant can be derived from the experimental data, of  $RD = 6 \times 10^{-13} \text{ cm}^3/\text{s}$  (see Supporting Information). This product is orders of magnitude too low for a classical diffusion process, which can be understood as follows. On one hand, one may take the exciton diffusion constant  $D > 0.3 \text{ cm}^2/\text{s}$ , as reported for bulk wurtzite CdSe at a temperature of 40 K.<sup>24</sup> This implies a reaction radius  $R < 2 \times 10^{-5} \text{ nm}$ , which is orders of magnitude below the dimension of an atom, representing the lowest possible reaction radius. Drawback of this argument is that the diffusion at room temperature is unknown. On the other hand, one may assume an exciton Bohr radius in infinitely thin nanoplatelets of about a factor 2 smaller than in bulk,<sup>25</sup> such that  $R = 3 \text{ nm}$ . This value leads to an exciton diffusion constant at room temperature of  $D = 2 \times 10^{-6} \text{ cm}^2/\text{s}$ . The diffusion constant is related to the velocity,  $v$ , of the center of mass of the exciton and the scattering length,  $\lambda$ , via  $D = v\lambda$ . Using the zero-point energy of an exciton with mass equal to the sum of the effective masses of an electron and a hole, moving in a two-dimensional box with dimensions of a nanoplatelet, yields a lower limit of  $v = 2 \times 10^4 \text{ m/s}$  for the velocity. This leads to an upper limit of the scattering length  $\lambda = 10^{-5} \text{ nm}$ , which is unrealistic since it much smaller than an interatomic spacing. On basis of the above, we conclude that Auger recombination in nanoplatelets does not occur via a *diffusion limited* mechanism. Moreover, it is likely that exciton diffusion does not occur at all in nanoplatelets, due to the fact that the wave function describing the center-of-mass motion of an exciton is delocalized throughout the nanoplatelet. Note the importance of distinguishing the center-of-mass wave function from that of the electron–hole difference coordinate: in our nanoplatelets, the center of mass wave function is delocalized through the nanoplatelet, and the difference coordinate wave function is localized.

Interestingly, the Auger recombination rate of biexcitons in the nanoplatelets is about 1 order of magnitude lower than for CdSe quantum dots and nanorods of equal volume.<sup>19,26,27</sup> This can be understood, since restrictions due to conservation of momentum and energy of electrons involved in the Auger process are more severe for systems of higher dimensionality. Such restrictions are even more important in three-dimensional bulk material. To the best of our knowledge, accurate data on the Auger recombination kinetics and rate have not been

reported for bulk CdSe, preventing comparison of the present results with those for bulk.

Auger recombination of electrons and holes in CdSe nanoplatelets can be described by bimolecular (second-order) kinetics. This implies that electrons and holes have a prevalently excitonic character, as opposed to free charges. The biexciton Auger recombination rate is more than 1 order of magnitude lower than for quantum dots or nanorods of equal volume. Slower Auger recombination is advantageous for application of nanoplatelets in lasers and light-emitting diodes. It also facilitates extraction of charge carriers from nanoplatelets in photovoltaic applications, in particular when carrier multiplication results in formation of multiple excitons in close proximity.

## ■ ASSOCIATED CONTENT

### Supporting Information

Theoretical model used to analyze the Auger recombination kinetics. This material is available free of charge via the Internet at <http://pubs.acs.org>.

## ■ AUTHOR INFORMATION

### Corresponding Authors

\*E-mail: L.D.A.Siebbeles@tudelft.nl.

\*E-mail: J.M.Schins@tudelft.nl.

### Notes

The authors declare no competing financial interest.

## ■ ACKNOWLEDGMENTS

This research was supported by the Dutch Foundation for Fundamental research on Matter (FOM), in the program "Control over Functional Nanoparticle Solids".

## ■ REFERENCES

- (1) Talapin, D. V.; Lee, J. S.; Kovalenko, M. V.; Shevchenko, E. V. Prospects of Colloidal Nanocrystals for Electronic and Optoelectronic Applications. *Chem. Rev.* **2010**, *110*, 389–458.
- (2) Krahne, R.; Morello, G.; Figuerola, A.; George, C.; Deka, S.; Manna, L. Physical Properties of Elongated Inorganic Nanoparticles. *Phys. Rep.* **2011**, *501*, 75–221.
- (3) Kubacka, A.; Fernández-García, M.; Colón, G. Advanced Nanoarchitectures for Solar Photocatalytic Applications. *Chem. Rev.* **2011**, *112*, 1555–1614.
- (4) Deka, S.; Quarta, A.; Lupo, M. G.; Falqui, A.; Boninelli, S.; Giannini, C.; Morello, G.; De Giorgi, M.; Lanzani, G.; Spinella, C.; Cingolani, R.; Pellegrino, T.; Manna, L. CdSe/CdS/ZnS Double Shell Nanorods with High Photoluminescence Efficiency and Their Exploitation as Biolabeling Probes. *J. Am. Chem. Soc.* **2009**, *131*, 2948–2958.
- (5) Kambhampati, P. Hot Exciton Relaxation Dynamics in Semiconductor Quantum Dots: Radiationless Transitions on the Nanoscale. *J. Phys. Chem. C* **2011**, *115*, 22089–22109.
- (6) Kambhampati, P. Unraveling the Structure and Dynamics of Excitons in Semiconductor Quantum Dots. *Acc. Chem. Res.* **2010**, *44*, 1–13.
- (7) Bouet, C.; Tessier, M. D.; Ithurria, S.; Nadal, B.; Mahler, B.; Dubertret, B. Flat Colloidal Semiconductor Nanoplatelets. *Chem. Mater.* **2013**, *25*, 1262–1271.
- (8) Xu, M.; Liang, T.; Shi, M.; Chen, H. Graphene-Like Two-Dimensional Materials. *Chem. Rev.* **2013**, *113*, 3766–3798.
- (9) Ithurria, S.; Tessier, M. D.; Mahler, B.; Lobo, R. P. S. M.; Dubertret, B.; Efros, A. L. Colloidal Nanoplatelets with Two-Dimensional Electronic Structure. *Nat. Mater.* **2011**, *10*, 936–941.
- (10) Achtstein, A. W.; Schliwa, A.; Prudnikau, A.; Hardzei, M.; Artemyev, M. V.; Thomsen, C.; Woggon, U. Electronic Structure and Exciton-Phonon Interaction in Two-Dimensional Colloidal CdSe Nanosheets. *Nano Lett.* **2012**, *12*, 3151–3157.
- (11) Pelton, M.; Ithurria, S.; Schaller, R. D.; Dolzhenkov, D. S.; Talapin, D. V. Carrier Cooling in Colloidal Quantum Wells. *Nano Lett.* **2012**, *12*, 6158–6163.
- (12) Pedetti, S.; Nadal, B.; Lhuillier, E.; Mahler, B.; Bouet, C.; Abecassis, B.; Xu, X.; Dubertret, B. Optimized Synthesis of CdTe Nanoplatelets and Photoresponse of CdTe Nanoplatelet Films. *Chem. Mater.* **2013**, *25*, 2455–2462.
- (13) Tessier, M. D.; Javaux, C.; Maksimovic, I.; Lorient, V.; Dubertret, B. Spectroscopy of Single CdSe Nanoplatelets. *ACS Nano* **2012**, *6*, 6751–6758.
- (14) de Mello Donega, C.; Koole, R. Size Dependence of the Spontaneous Emission Rate and Absorption Cross Section of CdSe and CdTe Quantum Dots. *J. Phys. Chem. C* **2009**, *113*, 6511–6520.
- (15) Iveland, J.; Martinelli, L.; Peretti, J.; Speck, J. S.; Weisbuch, C. Direct Measurement of Auger Electrons Emitted from a Semiconductor Light-Emitting Diode under Electrical Injection: Identification of the Dominant Mechanism for Efficiency Droop. *Phys. Rev. Lett.* **2013**, *110*, 177406.
- (16) Padilha, L. A.; Stewart, J. T.; Sandberg, R. L.; Bae, W. K.; Koh, W.-K.; Pietryga, J. M.; Klimov, V. I. Carrier Multiplication in Semiconductor Nanocrystals: Influence of Size, Shape, and Composition. *Acc. Chem. Res.* **2013**, *46*, 1261–1269.
- (17) Klimov, V. I.; Mikhailovsky, A. A.; Xu, S.; Malko, A.; Hollingsworth, J. A.; Leatherdale, C. A.; Eisler, H. J.; Bawendi, M. G. Optical Gain and Stimulated Emission in Nanocrystal Quantum Dots. *Science* **2000**, *290*, 314–317.
- (18) Landsberg, P. *Recombination in Semiconductors*; Cambridge University Press: Cambridge, U.K., 1991.
- (19) Htoon, H.; Hollingsworth, J. A.; Dickerson, R.; Klimov, V. I. Effect of Zero- to One-Dimensional Transformation on Multiparticle Auger Recombination in Semiconductor Quantum Rods. *Phys. Rev. Lett.* **2003**, *91*, 227401.
- (20) Mahler, B.; Nadal, B.; Bouet, C.; Patriarche, G.; Dubertret, B. Core/Shell Colloidal Semiconductor Nanoplatelets. *J. Am. Chem. Soc.* **2012**, *134*, 18591–18598.
- (21) Tessier, M. D.; Mahler, B.; Nadal, B.; Heudin, H.; Pedetti, S.; Dubertret, B. Spectroscopy of Colloidal Semiconductor Core/Shell Nanoplatelets with High Quantum Yield. *Nano Lett.* **2013**, *13*, 3321–3328.
- (22) Barzykin, A. V.; Tachiya, M. Stochastic Models of Charge Carrier Dynamics in Semiconducting Nanosystems. *J. Phys.: Condens. Matter* **2007**, *19*, 065105.
- (23) Barzykin, A.; Tachiya, M. Stochastic Models of Carrier Dynamics in Single-Walled Carbon Nanotubes. *Phys. Rev. B* **2005**, *72*, 075425.
- (24) Madelung, O.; Rössler, U.; Schulz, M. *Landolt-Börnstein - Group III Condensed Matter, Vol. 41B: Cadmium selenide (CdSe) hole mobility, carrier and ion diffusion*; Springer-Verlag: Berlin/Heidelberg/New York, 1999.
- (25) Haug, H.; Koch, S. W. *Quantum Theory of the Optical and Electronic Properties of Semiconductors*; World Scientific: Singapore, 1994.
- (26) Taguchi, S.; Saruyama, M.; Teranishi, T.; Kanemitsu, Y. Quantized Auger Recombination of Biexcitons in CdSe Nanorods Studied by Time-Resolved Photoluminescence and Transient-Absorption Spectroscopy. *Phys. Rev. B* **2011**, *83*, 155324.
- (27) Zhu, H.; Lian, T. Enhanced Multiple Exciton Dissociation from CdSe Quantum Rods: The Effect of Nanocrystal Shape. *J. Am. Chem. Soc.* **2012**, *134*, 11289–11297.